ELSEVIER

Journal of Molecular Structure 602–603 (2002) 417–428

Journal of
MOLECULAR
STRUCTURE

www.elsevier.com/locate/molstruc

A conformational study of aromatic imide compounds. Part 2. Compounds containing diphenyl sulfide, diphenyl sulfone, and diphenylmethane moieties ☆

Keitaro Aimi, Akira Yamane, Shinji Ando*

Department of Organic and Polymeric Materials, Tokyo Institute of Technology, Ookayama, Meguro-ku, Tokyo 152-8552, Japan

Received 21 March 2001; accepted 4 April 2001

Abstract

An attempt was made to estimate the dihedral angles, ϕ, ψ, ω_1, and ω_2, of bis(4-hydroxyphthalimide)s (BHPI) and bis(phenylphthalimide)s (BPI) having diphenyl sulfide, diphenyl sulfone, or diphenylmethane linkages at the center of molecules using solid–state ^{13}C CP/MAS NMR and *ab initio* nuclear shielding calculations. The TOSS and TOSS & DD pulse sequences were performed in the NMR measurements to obtain exact chemical shifts of each carbon. Total energies were calculated using the B3LYP/6-31G(d) level of theory, and shielding constants were calculated using the RHF/6-31G(d) level of theory for diphenyl sulfide, diphenyl sulfone, diphenylmethane with varying angles of ϕ, ψ from 0 to 180° at intervals of 10°. It was clarified that the –S– and $-SO_2-$ linkages lead asymmetrical conformations with different ω_1 and ω_2 or with different ϕ and ψ for BHPIs and BPIs. In contrast, the compounds having $-CH_2-$ linkages have symmetrical conformations. The dihedral angle of imide ring and phenylene ring (ω) are in the range of 40–90°, and the dihedral angles (ϕ, ψ) distribute in the stable regions of the energy surfaces ranging from 40 to 90°.

Keywords: CP/MAS NMR; Shielding constant; Dihedral angle; Diphenyl structure; Polyimide

1. Introduction

In Part 1 of this series [1], we have estimated the dihedral angles of BHPIs, BPIs, and ODPA/ODA polyimide that have diphenyl ether (DPO) and benzophenone (DPCO) linkages at the center of molecules or in the repeating unit. From the results of shielding constant calculations, it was clarified that the number of peaks of the carbons in diphenyl region is determined by the relationship between the two dihedral angles, ϕ and ψ. That is to say, when the signal of a certain carbon is singlet, two dihedral angles ϕ and ψ are identical, otherwise, they are different. Moreover, dihedral angles can be estimated by comparing ^{13}C NMR chemical shift differences between phenyl carbons with variations in calculated nuclear shieldings. For all the compounds we studied, the dihedral angles at diphenyl linkages were estimated as $\phi = \psi$, and the dihedral angles distributes in the stable regions of the energy surfaces ranging from 30 to 90°. In addition, the dihedral angle ω ranges between 45 and 90°. In this article, we estimate the conformations of the BHPIs and BPIs that have diphenyl sulfide (DPS), diphenyl sulfone ($DPSO_2$), diphenylmethane

☆ Dedicated to Professor Graham A. Webb on the occasion of his 65th birthday.

* Corresponding author. Tel.: +81-3-5734-2137; fax: +81-3-5734-2889.

E-mail address: sando@polymer.titech.ac.jp (S. Ando).

0022-2860/02/$ - see front matter
PII: S0022-2860(01)00709-8

(a) BHPI

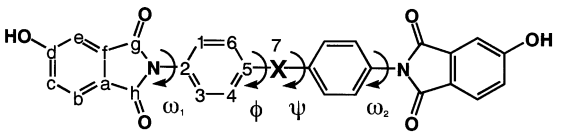

X = –S–, –SO_2– and –CH_2–

(b) BPI

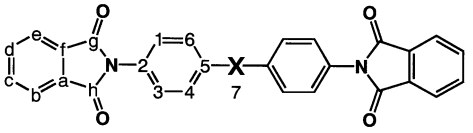

X = –S–, –SO_2– and –CH_2–

(c) *N*-phenylphthalimide (NPPI)

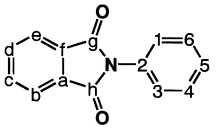

Scheme 1.

($DPCH_2$) linkages at the center of molecules. These diphenyl linkages frequently appear in high-performance engineering plastics.

2. Experimental

2.1. Synthesis

The general formula of BHPI and BPI are shown in Scheme 1. Two BHPIs that have central linkages of –SO_2– (*N*,*N*′-(4,4′-sulfonyldiphenylene)-bis-(5-hydroxy-2-phenyl-isoindole-1,3-dione), BHPI-$DPSO_2$) and –CH_2– (*N*,*N*′-(4,4′-methylidenediphenylene)-bis-(5-hydroxy-2-phenyl-isoindole-1,3-dione), BHPI-$DPCH_2$) were provided by NTT corporation. *N*,*N*′-(4,4′-sulfanyldiphenylene)-bis-(5-hydroxy-2-phenyl-isoindole-1,3-dione) (BHPI-DPS) that has the central linkage of –S– was synthesized according to the literature [2]. In order to exclude the effect of intermolecular hydrogen bonding, three bisphenylenephthalimide (*N*,*N*′-(4,4′-sulfanyldiphenylene)-bis-(2-phenyl-isoindole-1,3-dione) (BPI-DPS), *N*,*N*′-(4,4′-sulfonyldiphenylene)-bis-(2-phenyl-isoindole-1,3-dione) (BPI-$DPSO_2$), and *N*,*N*′-(4,4′-methylidenediphenylene)-bis-(2-phenyl-isoindole-1,3-dione) (BPI-$DPCH_2$)), which have the same skeletal structures as those of BHPI but no hydroxyl groups, were also synthesized

As an example, the synthesis of BHPI-DPS is described as follows: a mixture containing 15.2 g of *N*-methyl-2-pyrrolidinone (NMP) and 7.6 g of *o*-xylene was added to 3.79 g (23.12 mmol) of 4-hydroxyphthalic anhydride and 2.50 g (11.56 mmol) of 4,4′-diaminodiphenyl sulfide. This mixture was then heated under reflux at 190°C for several hours to remove the water of reaction by azeotropic distillation. The mixture was allowed to stand at room temperature and poured into methanol. The solid product was filtered out and rinsed with acetone, and dried in a vacuum at 100°C for 6 h. The obtained BHPI-DPS was 5.35 g (91.0% yield). BPIs were synthesized in the same manner except for using phthalic anhydride instead of 4-hydroxyphthalic anhydride. BHPI-DPS and BHPI-$DPCH_2$ were recrystalized from tetrahydrofuran (THF), and BHPI-$DPSO_2$ was recrystalized from acetone. All BPI samples were recrystalized from chloroform.

2.2. NMR measurements

Solution state ^{13}C NMR spectra were observed with JEOL GSX-500 spectrometer operating at 125 MHz. Dimethylsulfoxide (DMSO-d_6) was used as a solvent for BHPIs, and chloroform-*d* was used for BPIs. The DEPT sequence was used for selective observation of protonated carbons. Tetramethylsilane (TMS) was used as the internal standard ($\delta_C = 0$ ppm).

Solid-state ^{13}C CP/MAS NMR spectra were observed with JEOL GSX-270 spectrometer operating at 67.8 MHz. The total suppression of spinning sideband (TOSS) pulse sequence was used to suppress spinning sidebands. The pulse sequence that combines TOSS and the dipolar dephasing (non-quaternary carbon suppression) (TOSS & DD) was also used for selective observation of the non-protonated carbons. The CP contact time was 2 ms, and the recycle delay was 5 s. The chemical shifts calibrated indirectly through the adamantane peak observed at lower frequency (29.5 ppm relative to TMS).

2.3. MO calculations

As mentioned in Part 1, the B3LYP/6-31G(d) level

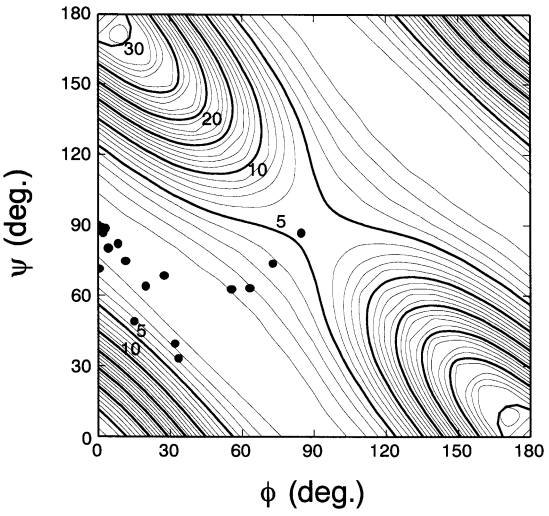

Fig. 1. Conformational energy surface of diphenyl sulfide (DPS) calculated using B3LYP/6-31G(d) level of theory. The dihedral angles of diphenyl sulfide structures reported for single crystals are plotted by filled circles within the range of $0° \leq \phi \leq 90°$ and $\psi \geq \phi$ (see text).

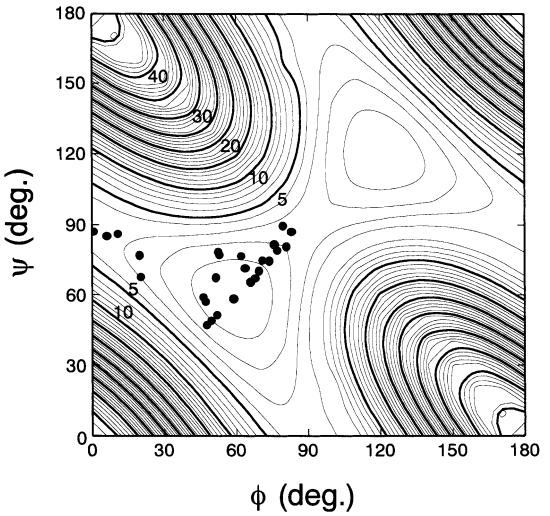

Fig. 3. Conformational energy surface of diphenylmethane ($DPCH_2$) calculated using B3LYP/6-31G(d) level of theory. The dihedral angles of diphenylmethane structures reported for single crystals are plotted in the same manner as in Fig. 1.

of theory was used for the calculation of conformational energies, and the RHF/6-31G(d) level of theory was used for the shielding constant calculations. The program package of molecular orbital theory used was GAUSSIAN 98 installed in the Computer Center of Tokyo Institute of Technology [3]. Two dihedral angles, ϕ and ψ (refer to Scheme 2 of Part 1) of diphenyl sulfide (DPS), diphenyl sulfone ($DPSO_2$), and diphenylmethane ($DPCH_2$) were varied from 0 to 180° at 10° intervals. Geometrical parameters (bond lengths and bond angles) were optimized for each conformation, followed by ^{13}C magnetic shielding calculation using GIAO-CHF method [4].

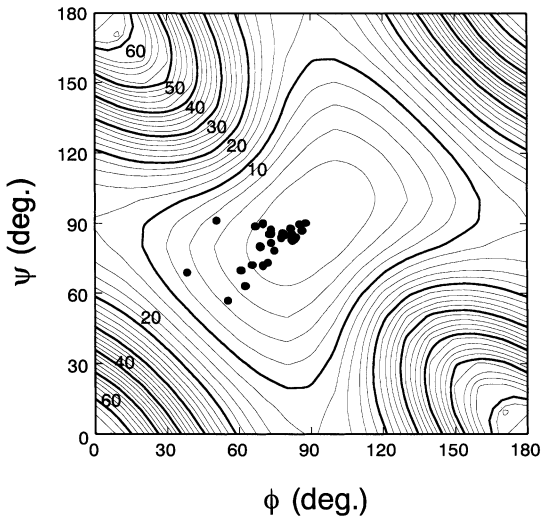

Fig. 2. Conformational energy surface of diphenyl sulfone ($DPSO_2$) calculated using B3LYP/6-31G(d) level of theory. The dihedral angles of diphenyl sulfone structures reported for single crystals are plotted in the same manner as in Fig. 1.

3. Results and discussion

3.1. Conformational energy surfaces

Figs. 1–3 show the conformation energy surfaces of DPS, $DPSO_2$ and $DPCH_2$, respectively. The intervals of lines in the energy contour maps are 1 kJ/mol in Figs. 1 and 3, and 2 kJ/mol in Fig. 2. Since the left and right halves of the energy surface are point-symmetrical with respect to the point of (90°,90°), we consider only the left half. The dihedral angles of diphenyl sulfide [5–22], diphenyl sulfone [23–41], and diphenylmethane [42–63] structures reported for single crystals are also plotted in Figs. 1–3. These data were collected from the Cambridge Structural

Database [64]. Since the benzene rings in DPO and DPCO have symmetrical structures, the conformation of (ϕ, ψ) is in principle same as that of (ψ, ϕ). Hence, the conformations of single crystals are plotted in the area of $\phi < \psi$.

The energy minima are found at $(\phi, \psi) = (30°, 60°)$ and (60°,30°) for DPS (Fig. 1). The large minimum region (<1 kJ/mol) extends from (0°,90°) to (90°,0°). The energy difference between the minimum point and (0°,90°) is 0.44 kJ/mol. This value is slightly smaller than that for DPO (0.67 kJ/mol, see Part 1). Hence, the transition accompanying the rotation of benzene rings between the two minimum points, i.e. (30°,60°) to (150°,120°), in which both are mutual enantiomers, passes the conformation of (0°,90°). On the other hand, the energy difference between the minimum point and (90°,90°) is 5.33 kJ/mol, which is much smaller than that of DPO (17.07 kJ/mol). Anwer et al. has reported a conformational energy surface and the energy minimum at (40°,40°) for DPS using MM2 calculation [65]. The overall surface shape obtained from MM2 is similar to that of Fig. 1. The energy minimum was reported as $(\phi, \psi) = (35°, 35°)$ for DPS from a semi-empirical (AM1) calculation [66]. These stable conformations also agree well with our results. Most of the dihedral angles of the single crystals having diphenyl sulfanyl linkages are located close to the minimum region and tend to distribute on the line of $\phi = \psi$ (Case A) or $\phi + \psi = 90°$ (Case B).

The energy minimum is found at (90°,90°) for $DPSO_2$ (Fig. 2), which agrees with those of MM2 calculation [65] and HF/3-21G level of theory [67]. The minimum region (<2 kJ/mol) extends from (70°,70°) to (110°,110°). The energy difference between the minimum point and (0°,90°) is 11.84 kJ/mol, which indicates that the energy barrier for the benzene ring rotation is very high for $DPSO_2$ compared to other diphenyl structures. Most of the dihedral angles of single crystals having diphenyl sulfone linkages are located in the minimum region.

The energy minimum is found at (60°,60°) for $DPCH_2$ (Fig. 3). The minimum region (<1 kJ/mol) ranges within 10° of (60°,60°). The energy difference between the minimum point and (0°,90°) is 3.13 kJ/mol, and that of (90°,90°) is 2.54 kJ/mol. This indicates that the transition accompanying the rotation of benzene rings between the two energy minima, i.e. (60°,60°) and (120°,120°), can pass both the transition states of (0°,90°) or (90°,90°). Straßner has reported conformational energy surfaces of $DPCH_2$ using AM1 methods and B3LYP/3-21G(d) level of theory [68]. According to his report, the energy minimum of $DPCH_2$ is located at (57°,57°), and it agrees with the high-level Hartree–Fock *ab initio* calculation (MP2) of 58.5° [69]. The shapes of the surfaces reported (HF/6-31G(d) [69] and B3LYP/3-21G(d) [68]) are almost identical to that of Fig. 3. The dihedral angles of single crystals having diphenylmethane linkages are located close to the minimum region and tend to distribute on the line of $\phi = \psi$ (Case A) or $\phi + \psi = 90°$ (Case B).

3.2. Shielding constant calculation

The surface shapes of the shielding constants for DPO was examined in Part 1 [1]. It was clarified that the shielding constants of diphenyl carbons significantly vary with the dihedral angles ϕ and ψ. In the case of $\phi = \psi$ (Case A), the shielding constants of symmetrical two carbons in different phenyl rings (C_x and $C_{x'}$) are identical, otherwise, they are different. Hence, the conformation of diphenyl region can be inferred from the number of peaks in NMR spectrum. Although the nuclear shieldings of all carbons show dihedral angle dependence, we selected the chemical shifts of C_4 and C_6 for estimating the dihedral angles from the reasons stated in the preceding paper [1].

Figs. 4–6 show the dihedral angle dependence of shielding constants of C_4 and C_6 for DPS, $DPSO_2$ and $DPCH_2$, respectively. In Case A, the shielding constants of C_4, C_6 and their difference ($\Delta_{4,6}$) significantly vary with the dihedral angles, and the dihedral angles can be estimated from the curve of $\Delta_{4,6}$. On the other hand, the difference between C_4 and $C_{5'}$ ($\Delta_{4,4'}$) was used for the estimation of dihedral angles in Case B because the dihedral angle dependence of $\Delta_{4,6}$ for DPS (Fig. 4b) and $DPCH_2$ (Fig. 6b) is very small.

3.3. Shielding constant calculation of NPPI

The dihedral angles ω is defined by the interring rotation of the imide ring and phenylene ring in BHPIs and BPIs. The chemical shifts of diphenyl carbons, C_1, C_2, C_3, and C_5 should be influenced by the dihedral angles ω_1 and ω_2. The chemical shifts of C_4 and C_6 are

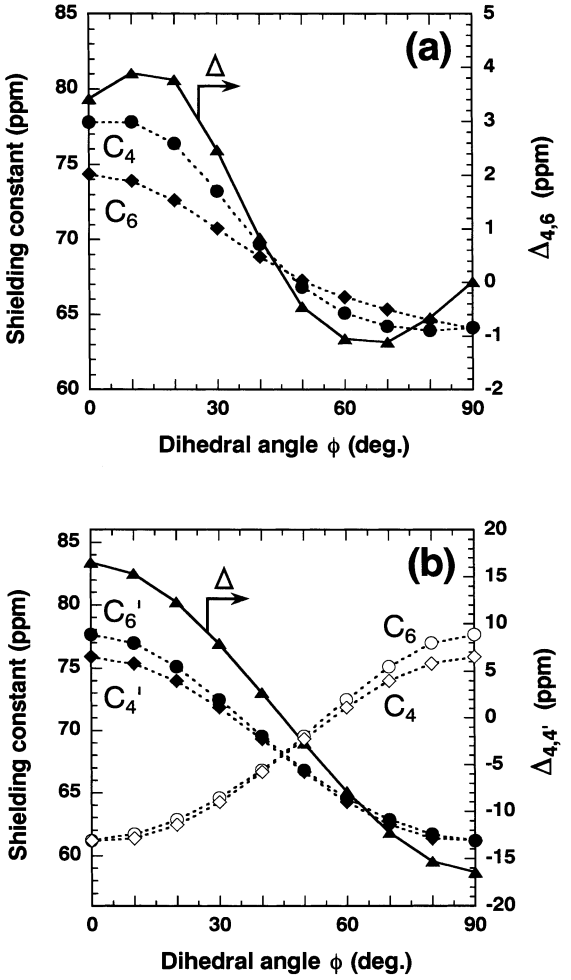

Fig. 4. Dihedral angles dependence of the shielding constants of diphenyl sulfide (DPS) for the cases of (a) $\phi = \psi$ (Case A) ($0° \leq \phi \leq 90°$), and (b) $\phi + \psi = 90°$ (Case B). The shielding constant difference between C_4 (σ_4) and C_6 (σ_6) is expressed as $\Delta_{4,6}$, and that between C_4 (σ_4) and C'_4 ($\sigma_{4'}$) is expressed as $\Delta_{4,4'}$.

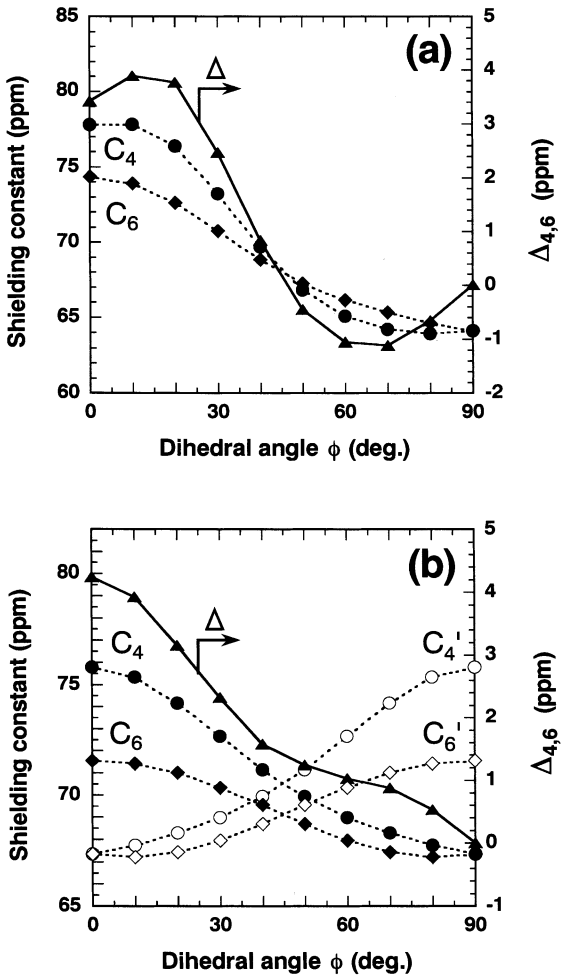

Fig. 5. Dihedral angle dependence of the shielding constants of diphenyl sulfone ($DPSO_2$) for (a) Case A and (b) Case B. The plots are in the same manner as in Fig. 4.

insensitive to the dihedral angle ω because they are located at the *meta*-positions. The shielding constants of *N*-phenylphthalimide (NPPI) were calculated to investigate the dihedral angle (ω) dependence of nuclear shieldings of such diphenyl carbons. The geometry of NPPI was optimized using B3LYP/6-31G(d) level of theory with varying ω at 10° intervals, and the shielding constants were calculated using RHF/6-31G(d) level of theory.

Fig. 7 shows the ω dependence of the shielding constants of phenyl carbons in NPPI. The shielding constant of C_1 shows a considerable decrease as the ω increases, whereas that of C_4 is insensitive to the variation of ω. The shielding constant of C_2 increases as the ω increases from 0 to 50°, and that of C_5 gently decreases as the ω increases. These results indicate that when the dihedral angles at imide-phenyl bonds (ω_1 and ω_2) of BHPI and BPI are different, two symmetrical carbons in different phenyl rings exhibit different chemical shifts. For example, when ω_1 is 40° and ω_2 is 90°, a displacement of ca. 6 ppm could be observed for the chemical shifts of C_1 and $C_{1'}$. Consequently, even if the dihedral angles ϕ and ψ take the same value, two split peaks can be observed for C_1,

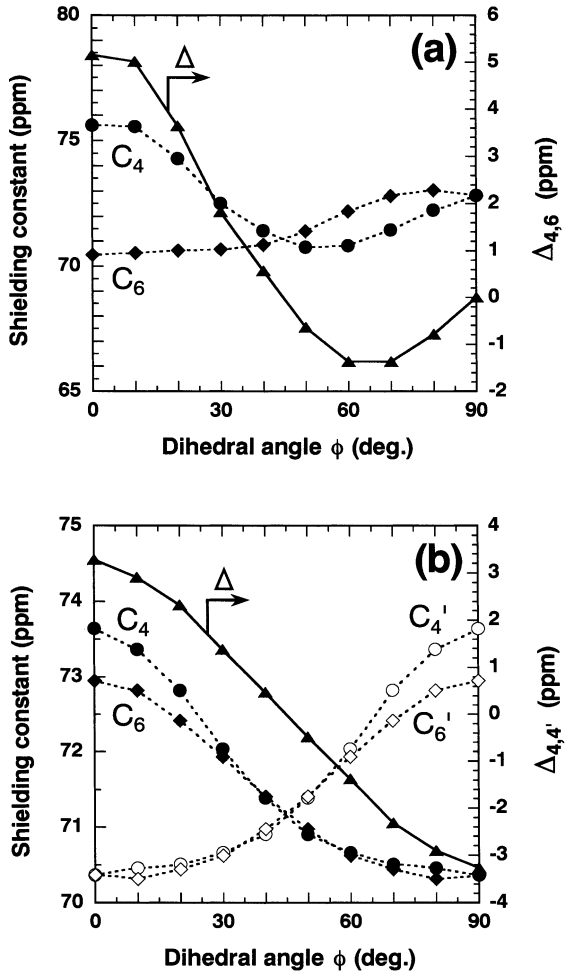

Fig. 6. Dihedral angle dependence of the shielding constants of diphenylmethane ($DPCH_2$) for (a) Case A and (b) Case B. The plots are in the same manner as in Fig. 4.

C_2, C_3, and C_5 when two dihedral angles ω_1 and ω_2 are different.

3.4. Estimation of dihedral angles

Dihedral angle ω can be estimated using the correlation between the chemical shift difference of solid-state and solution-state chemical shifts ($\Delta_{\text{solid–solution}}$) for C_1 carbon and the dihedral angles determined by X-ray crystallography [70]. The dihedral angle ω can be estimated by applying a value of $\Delta_{\text{solid–solution}}$ for the correlation curve in Fig. 7 of Part 1.

Figs. 8–13 show the ^{13}C solution-state NMR and

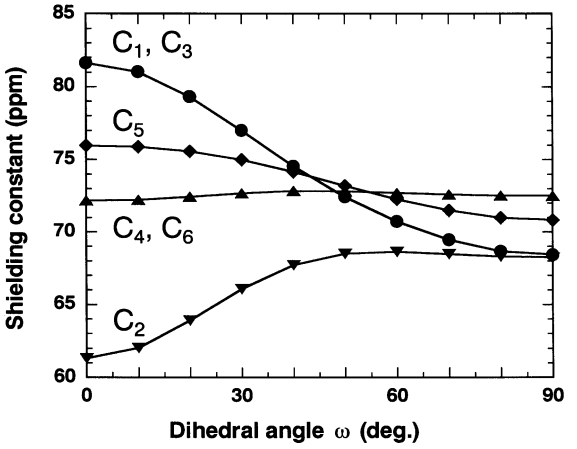

Fig. 7. Dihedral angle (ω) dependence of the shielding constants of phenyl carbons of *N*-phenylphthalimide. The numbers of carbons correspond to those in Scheme 1.

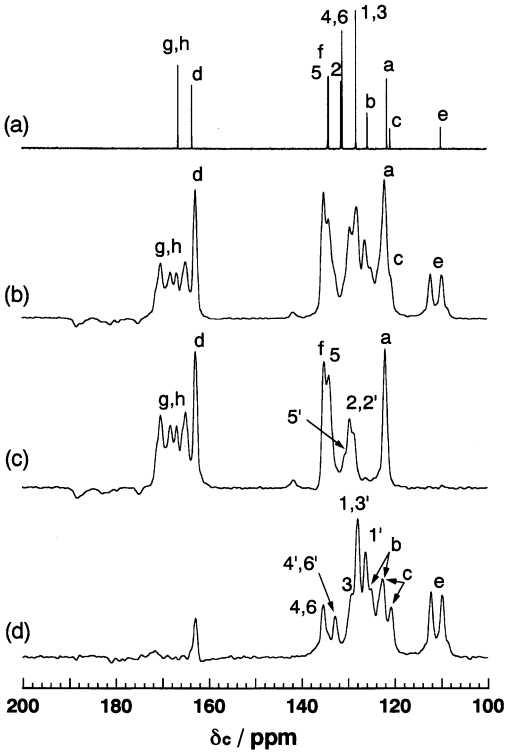

Fig. 8. (a) Solution, (b) TOSS, (c) TOSS & DD and (d) subtracted (c from b) NMR spectra and signal assignments of BHPI-DPS. Symbols in the spectra correspond to the carbons shown in Scheme 1.

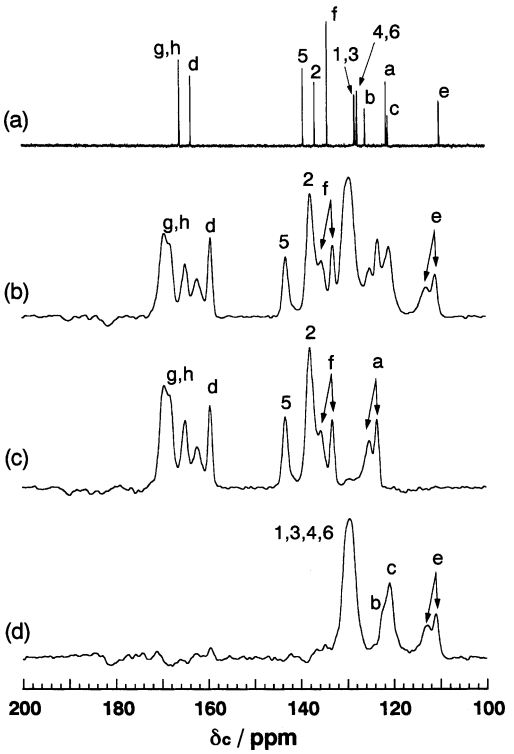

Fig. 9. (a) Solution, (b) TOSS, (c) TOSS & DD and (d) subtracted (c from b) NMR spectra and signal assignments of BHPI-DPSO$_2$.

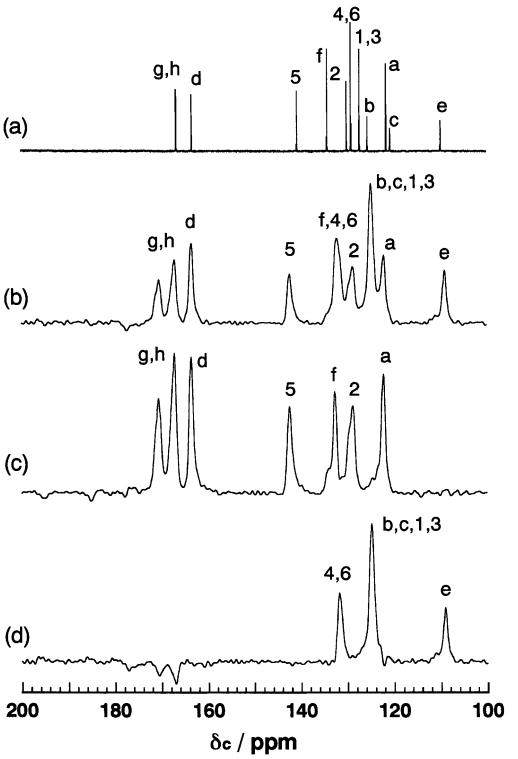

Fig. 10. (a) Solution, (b) TOSS, (c) TOSS & DD and (d) subtracted (c from b) NMR spectra and signal assignments of BHPI-DPCH$_2$.

solid-state CP/MAS NMR spectra of BHPI-DPS, BHPI-DPSO$_2$, BHPI-DPCH$_2$, BPI-DPS, BPI-DPSO$_2$ and BPI-DPCH$_2$, respectively, together with their signal assignments. The peaks of solution-state NMR spectra were assigned using the substituent shielding effects on benzene and related compounds [71]. The peaks of solid-state NMR spectra were assigned by referring to the assignment of solution-state spectra. The peak positions expected from the shielding constant calculations were also used to assign the signals in diphenyl region. The dihedral angles, ω_1, ω_2, ϕ and ψ of each sample are estimated in the following.

3.4.1. BHPI-DPS

For symmetrical molecular conformations with the same ϕ and ψ and the same ω_1 and ω_2, the signals of carbons located at symmetrical positions in the phenyl rings of BHPI and BPI (C_x and $C_{x'}$) should be singlet as mentioned above. In the TOSS & DD spectrum of BHPI-DPS (Fig. 8c), split peaks are observed for C_2 and C_5. Split peaks are also observed for the other diphenyl carbons in subtracted spectrum (Fig. 8d). Considering the number of peaks in Fig. 8, BHPI-DPS should have an asymmetric conformation, in which the values of ϕ and ψ are different. The plots of single crystal structures in Fig. 1 show that most of the asymmetric DPS structures have nearly Case B structures ($\phi + \psi = 90°$). Hence, we assumed that $\phi + \psi = 90°$ for BHPI-DPS. The signals in the TOSS spectrum (Fig. 8b) are overlapped with each other, but the peaks at 126.2, 127.9, 127.9 and 129.5 ppm are assigned to C_1, C_3, $C_{1'}$ and $C_{3'}$, respectively, from the peak fitting using Lorentzian functions (the fitted spectrum is not shown). Furthermore, the average chemical shifts of C_1 and C_3 ($\delta_{1,3.\mathrm{solid}}$) and $C_{1'}$ and $C_{3'}$ ($\delta_{1',3'.\mathrm{solid}}$) were used for the estimation of the dihedral angle ω. The $\Delta_{1,3.\mathrm{solid-solution}}$ value of -0.9 ppm corresponds to $\omega = 55 \pm 5°$, and the $\Delta_{1',3'.\mathrm{solid-solution}}$ value of 0.7 ppm corresponds to $\omega = 70 \pm 5°$. From the subtracted

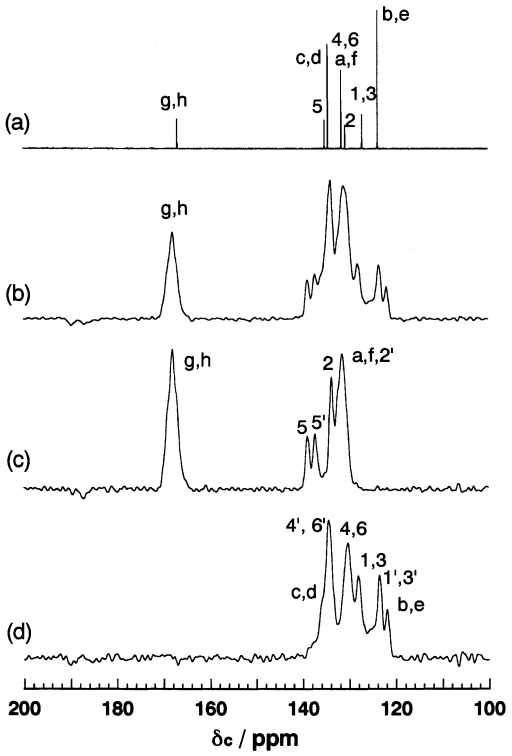

Fig. 11. (a) Solution, (b) TOSS, (c) TOSS & DD and (d) subtracted (c from b) NMR spectra and signal assignments of BPI-DPS.

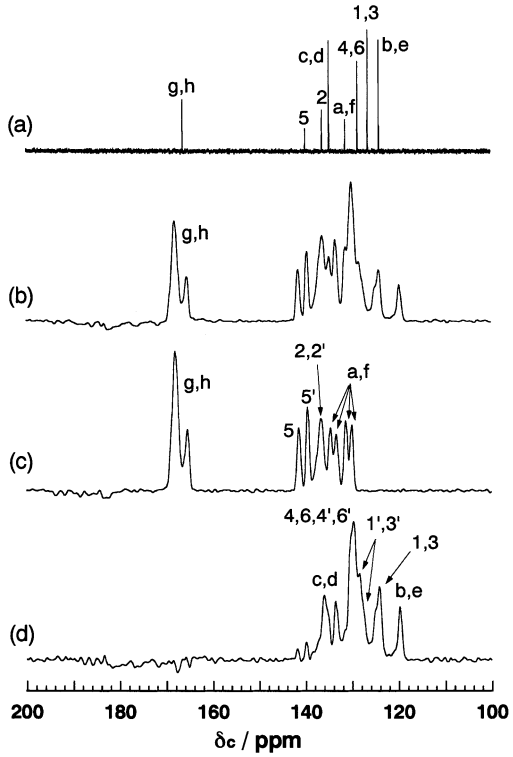

Fig. 12. (a) Solution, (b) TOSS, (c) TOSS & DD and (d) subtracted (c from b) NMR spectra and signal assignments of BPI-$DPSO_2$.

spectrum of Fig. 8d, the chemical shift difference between C_4 (135.3 ppm) and C'_4 (132.8 ppm) was estimated as $\Delta_{4,4'} = 2.5$ ppm. By applying this value to the curve in Fig. 4b, the dihedral angles are estimated as $(\phi, \psi) = (40 \pm 5°, 50 \pm 5°)$.

3.4.2. BHPI-$DPSO_2$

Single peaks observed for C_2 or C_5 in the TOSS & DD spectrum (Fig. 9c) indicates that the dihedral angles of ϕ and ψ are identical for BHPI-$DPSO_2$. In addition, since only single broad peak of C_1, C_3, C_4 and C_6 is observed in the subtracted spectrum (Fig. 9d), the dihedral angles ω_1 and ω_2 are also estimated to be identical. The peak splittings observed for C_a and C_f should originate from intermolecular interaction such as molecular packing effect because these carbons are insensitive to the conformational change. The value of $\Delta_{\text{solid–solution}}$ was estimated as 1.4 ppm from $\delta_{\text{solid}} = 129.4$ ppm and $\delta_{\text{solution}} = 128.0$ ppm in Fig. 9a and d. Hence, the dihedral angle ω is estimated as $90 \pm 5°$. On the other hand, the signals of C_4 and C_6 are overlapped with each other, and the value of $\Delta_{4,6}$ is estimated to be smaller than 1 ppm, which indicates that the dihedral angles ϕ and ψ are larger than 60° by applying this value to Fig. 5a.

3.4.3. BHPI-$DPCH_2$

Single peaks are observed for C_2 and C_5 in the TOSS & DD spectrum (Fig. 10c). The other diphenyl carbons also show single peaks in the subtracted spectrum (Fig. 10d). These results indicate that the dihedral angles of ϕ and ψ are identical for BHPI-$DPCH_2$. The solution-state chemical shift of C_1 is 127.1 ppm (Fig. 10a), and the solid-state chemical shift of C_1 and C_3 is 124.9 ppm (Fig. 10d). The value of $\Delta_{1,3.\text{solid–solution}}$ (-2.2 ppm) thus obtained corresponds to $\omega = 40 \pm 5°$. Since only one peak is observed for C_4 and C_6 at 132.3 ppm, the dihedral angles of ϕ and ψ are estimated as $(\phi, \psi) = (45 \pm 5°, 45 \pm 5°)$ or $(90 \pm 5°,\ 90 \pm 5°)$ by applying the value of $\Delta_{4,6}$ (0 ppm) to Fig. 6a. In the calculated energy surface of $DPCH_2$ (Fig. 3), both structures are possible.

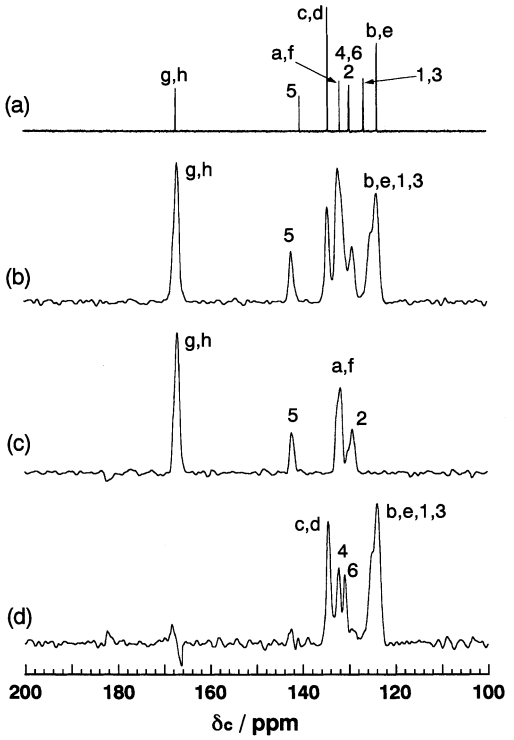

Fig. 13. (a) Solution, (b) TOSS, (c) TOSS & DD and (d) subtracted (c from b) NMR spectra and signal assignments of BPI-DPCH$_2$.

3.4.4. BPI-DPS

Split peaks are observed for C_2 and C_5 in the TOSS & DD spectrum (Fig. 11c), and split peaks are also observed for the other diphenyl carbons in the subtracted spectrum (Fig. 11d). Considering the number of peaks in Fig. 11, BPI-DPS should have an asymmetric structure. The chemical shift of C_1 in solution is 126.8 ppm in Fig. 11a, and the solid-state chemical shift of C_1 and $C_{1'}$ are 127.9 ppm and 123.5 ppm, respectively. The values of $\Delta_{1,3.\mathrm{solid-solution}}$ (-3.3 and 1.5 ppm) thus obtained correspond to $\omega_1 = 40 \pm 5°$ and $\omega_2 = 75 \pm 5°$. Furthermore, the $\Delta_{4,4'}$ value of 4.1 ppm is obtained from the subtracted spectrum (Fig. 11d). The dihedral angles of ϕ and ψ are estimated as $(\phi, \psi) = (38 \pm 5°, 52 \pm 5°)$ by applying the value of $\Delta_{4,4'}$ to Fig. 4b.

3.4.5. BPI-DPSO$_2$

The split peaks for C_5 (Fig. 12c) and protonated diphenyl carbons (Fig. 12d) indicate that BPI-DPSO$_2$ should have an asymmetric structure. Although splittings of peaks are observed for C_2 and C_5 in Fig. 12c, the calculated shielding constants of the diphenyl carbons are inconsistent with Case B taking account of the peak positions in NMR spectra. Hence, we assumed that these splittings originate not from the difference in ϕ and ψ, but from the difference in ω_1 and ω_2. As shown in Fig. 7, when the range of ω is limited between 40 and 90°, a maximum displacement of 3 ppm to lower frequency can be induced for C_5 by the difference in ω, but a displacement of less than 1 ppm can be induced for C_2. The spectral shapes of C_2 and C_5 observed in the TOSS & DD spectrum of Fig. 12c agree with this calculation: two split peaks are observed for C_5, whereas one broad peak is observed for C_2.

The chemical shift of C_1 in solution ($\delta_{\mathrm{solution}}$) is 126.3 ppm. Two dihedral angles ω_1 and ω_2 were estimated from the difference between $\delta_{\mathrm{solution}}$ and $\delta_{1,3.\mathrm{solid}}$ (124.1 ppm) and that between $\delta_{\mathrm{solution}}$ and $\delta_{1',3'.\mathrm{solid}}$ (128.5 ppm). The $\Delta_{1,3.\mathrm{solid-solution}}$ values of -2.2 and $+2.2$ ppm correspond to $\omega_1 = 50 \pm 5°$, and $\omega_2 = 90 \pm 5°$, respectively.

The dihedral angles ϕ and ψ are estimated to be larger than 60° by applying the value of $\Delta_{4,6}$ (less than 1 ppm) to Fig. 5a. Considering the chemical shift difference between C_5 and $C_{5'}$ ($\Delta_{5,5'}$), the ϕ and ψ are limited to the region around (90°,90°). When the dihedral angles, ω_1, and ω_2, are 50 and 90° as estimated above, the value of $\Delta_{5,5'}$ could be 2 ppm in Fig. 7. This agrees well with the experimental difference between C_5 (141.5 ppm) and C'_5 (139.8 ppm).

3.4.6. BPI-DPCH$_2$

The dihedral angles, ϕ and ψ are estimated to be identical because singlet peaks are observed for diphenyl carbons of BPI-DPCH$_2$ as seen in Fig. 13c and d. The $\Delta_{\mathrm{solid-solution}}$ value of -2.5 ppm, which is obtained from the solution-state and solid-state chemical shift of C_1 (126.4 and 123.9 ppm) corresponds to $\omega = 45 \pm 5°$. The dihedral angle ϕ and ψ are estimated as $(\phi, \psi) = (58 \pm 5°, 58 \pm 5°)$ by applying the value of $\Delta_{4,6}$ (1.2 ppm) to Fig. 6a.

Table 1 summarizes the dihedral angles, ω, ϕ and ψ, thus estimated above. Comparing the estimated values of ϕ and ψ with the conformational energy surfaces, $(\phi, \psi) = (40°, 50°)$ of BHPI-DPS and (38°,52°) of BPI-DPS are located in the most stable

Table 1
Estimated dihedral angles ω, ϕ and ψ, and relations between two dihedral angles ϕ and ψ.

Sample		Case[a]	ω (°)	(ϕ, ψ) (°)
BHPI	DPS	B	55 ± 5, 70 ± 5	$(40 \pm 5, 50 \pm 5)$
	$DPSO_2$	A	90 ± 5	60–90
	$DPCH_2$	A	40 ± 5	$(45 \pm 5, 45 \pm 5)$ or $(90 \pm 5, 90 \pm 5)$
BPI	DPS	B	40 ± 5, 75 ± 5	$(38 \pm 5, 52 \pm 5)$
	$DPSO_2$	A	50 ± 5, 90 ± 5	$(90 \pm 5, 90 \pm 5)$
	$DPCH_2$	A	45 ± 5	$(58 \pm 5, 58 \pm 5)$

[a] In case A, $\phi = \psi$, and in case B, $\phi + \psi = 90°$.

region of DPS (Fig. 1). Furthermore, the estimated conformations of $\phi = \psi > 60°$ for BHPI-$DPSO_2$ and $(\phi, \psi) = (90°, 90°)$ for BPI-$DPSO_2$ are located in the stable conformation of $DPSO_2$. The estimated conformation of (58, 58) for BPI-$DPCH_2$ is also located in the most stable region of $DPCH_2$ (Fig. 3). Although we cannot choose unique conformation of BHPI-$DPCH_2$, two possible conformations ((45°,45°) and (90°,90°)) are located in the slightly unstable regions (about 3 kJ/mol higher than the energy minimum). The examination of the conformations stated above clearly shows that the introduction of –S– and –SO_2– linkages to the center of molecules lead to asymmetrical conformations of BHPI and BPI, while the introduction of –CH_2– linkages provides symmetric conformations.

4. Conclusions

^{13}C NMR chemical shifts in the solution and solid states were used to investigate the conformation of BHPIs and BPIs having diphenyl sulfide, diphenyl sulfone, and diphenylmethane linkages. The dihedral angles ϕ, ψ, ω_1, and ω_2 were estimated by comparing the ^{13}C NMR chemical shift differences of phenyl carbons with the variations in the calculated shielding constants. It was clarified that the introduction of –S– and –SO_2– linkages at the center of BHPIs and BPIs leads to asymmetrical conformations with different ω_1 and ω_2 or ϕ and ψ. In contrast, the introduction of –CH_2– linkage leads to symmetric conformations. The range of the dihedral angle between imide and phenyl rings (ω) is between 40 and 90°, and the dihedral angles (ϕ, ψ) distribute in the stable regions of the energy surfaces ranging from 40 to 90°.

Acknowledgements

We wish to thank S. Sasaki and T. Matsuura at NTT for providing 4-hydroxyphthalimide and bis(4-hydroxyphthalimide)s.

References

[1] K. Aimi, T. Fujiwara, S. Ando, J. Mol. Struct. 602–603 (2002) 405–416.
[2] S. Sasaki, Y. Hasuda, J. Polym. Sci. Polym. Lett. 25 (1987) 377.
[3] M.J. Frisch, G.W. Trucks, H.B. Schlegel, G.E. Scuseria, M.A. Robb, J.R. Cheeseman, V.G. Zakrzewski, J.A. Montgomery, R.E. Stratmann Jr., J.C. Burant, S. Dapprich, J.M. Millam, A.D. Daniels, K.N. Kudin, M.C.C. Strain, O. Farkas, J. Tomasi, V. Barone, M. Cossi, R. Cammi, B. Mennucci, C. Pomelli, C. Adamo, S. Clifford, J. Ochterski, G.A. Petersson, P.Y. Ayala, Q. Cui, K. Morokuma, D.K. Malick, A.D. Rabuck, K. Raghavachari, J.B. Foresman, J. Cioslowski, J.V. Ortiz, A.G. Baboul, B.B. Stefanov, G. Liu, A. Liashenko, P. Piskorz, I. Komaromi, R. Gomperts, R.L. Martin, D.J. Fox, T. Keith, M.A. Al-Laham, C.Y. Peng, A. Nanayakkara, C. Gonzalez, M. Challacombe, P.M.W. Gill, B. Johnson, W. Chen, M.W. Wong, J.L. Andres, C. Gonzalez, M. Head-Gordon, E.S. Replogle, J.A. Pople, GAUSSIAN 98, Revision A.9, Gaussian, Inc., Pittsburgh, PA, 1998.
[4] R. Ditchfield, Mol. Phys. 27 (1974) 789.
[5] A. Kucsman, I. Kapovits, L. Parkanyi, G. Argay, A. Kalman, J. Mol. Struct. 125 (1984) 331 [CULFAQ10].
[6] L.A. Chetkina, V.E. Zavodnik, V.K. Bel'skii, I.G. Arzamanova, M.I. Naiman, Ya.G. Gurvich, Zh. Strukt. Khim. 25 (1984) 114 [DABMOI].
[7] B.K. Vijayalakshmi, R. Srinivasan, J. Cryst. Mol. Struct. 3 (1973) 147 [DAPHSD].
[8] K. von Deuten, G. Klar, Cryst. Struct. Commun. 10 (1981) 231 [DMOPHS].
[9] M. Sacerdoti, V. Bertolasi, G. Gilli, Cryst. Struct. Commun. 5 (1976) 477 [DOTOLS].
[10] N. Goodhand, T.A. Hamor, J. Fluor. Chem. (1979) 223 [DTFNPS].
[11] H. Abdel-Halim, D.O. Cowan, D.W. Robinson, F.M. Wiygul, M. Kimura, J. Phys. Chem. 90 (1986) 5654.
[12] M. Ratajczak-Sitarz, A. Katrusiak, Z. Kaluski, J. Garbarczyk, Acta Crystallogr., Sect.C: Cryst. Struct. Commun. 44 (1988) 315 [GAHGUR].

[13] R. Minkwitz, H. Preut, J. Sawatzki, Z. Anorg. Allg. Chem. 569 (1989) 158 [KAHVEU].
[14] H. Song, E. Kim, H.S. Shin, Bull. Korean Chem. Soc. 11 (1990) 19 [KESXIP].
[15] G. Bandoli, D.A. Clemente, E. Tondello, A. Dondoni, J. Chem. Soc., Perkin Trans. 2 (1974) 157 [MAMPHS10].
[16] A. Krajewski, L. Riva di Sanseverino, A. Dondoni, A. Mangini, J. Cryst. Mol. Struct. 5 (1975) 345 [NMADPS].
[17] J.D. Korp, I. Bernal, G.E. Martin, J. Cryst. Mol. Struct. 11 (1981) 11 [NOPHTE01].
[18] N. Goodhand, T.A. Hamor, Acta Crystallogr., Sect. C: Cryst. Struct. Commun. 45 (1989) 1609 [SAXKIL].
[19] W.R. Blackmore, S.C. Abrahams, Acta Crystallogr. 8 (1955) 329 [TOLSUL].
[20] L. Parkanyi, A. Kalman, A. Kucsman, I. Kapovits, J. Mol. Struct. 198 (1989) 355 [VEPCUO].
[21] T. Link, I. Eggers, G. Klar, J. Chem. Res. 90 (1995) 667 [YOYVAJ].
[22] R.A. Howie, J.L. Wardell, Acta Crystallogr., Sect. C: Cryst. Struct. Commun. 52 (1996) 1228 [ZUZYEY].
[23] J.G. Sime, D.I. Woodhouse, J. Cryst. Mol. Struct. 4 (1974) 287 [BPHSUL01].
[24] V.K. Bel'skii, N.Yu. Chernikova, V.K. Rotaru, M.M. Kruchinin, Kristallografiya 28 (1983) 690 [CEGYIW].
[25] G.E. Bacon, N.A. Curry, Acta Crystallogr. 13 (1960) 10 [CLPSUL01].
[26] F.J. Zuniga, J.M. Perez-Mato, T. Breczewski, Acta Crystallogr., Sect. B (Struct. Sci.) 49 (1993) 1060 [CLPSUL02].
[27] G. Bocelli, A. Cantoni, Acta Crystallogr., Sect. C: Cryst. Struct. Commun. 46 (1990) 2257 [DAPSUO03].
[28] G.-B. Su, F. Pan, Y.-P. He, S.-W. Guo, Chin. J. Struct. Chem. (Jiegou Huaxue) 11 (1992) 293 [DAPSUO04].
[29] V. Bertolasi, V. Ferretti, P. Gilli, P.G. De Benedetti, J. Chem. Soc., Perkin Trans. 2 (1993) 213 [DAPSUO05].
[30] M. Alleaume, Thesis, Bordeaux (1967) 49 [DAPSUO10].
[31] S.A. Chawdhury, A. Hargreaves, Acta Crystallogr., Sect. B 27 (1971) 548 [HMPSUL].
[32] J.G. Sime, D.I. Woodhouse, J. Cryst. Mol. Struct. 4 (1974) 269 [NFPHSO].
[33] J. Jeyakanthan, D. Velmurugan, K. Panneerselvam, M. Soriano-Garcia, S. Perumal, R. Chandrasekaran, Acta Crystallogr., Sect. C: Cryst. Struct. Commun. 54 (1998) 630 [NOFVUZ].
[34] J. Jeyaraman, D. Velmurugan, Acta Crystallogr., Sect. C: Cryst. Struct. Commun. 53 (1997) 1344 [RIWRUK].
[35] C. Davies, R.F. Langler, C.V.K. Sharma, M.J. Zaworotko, Chem. Commun. (1997) 567 [RIYVIE].
[36] K. Okada, J. Mol. Struct. 380 (1996) 223 [SIBQEZ].
[37] C. Glidewell, G. Ferguson, Acta Crystallogr., Sect. C: Cryst. Struct. Commun. 52 (1996) 2528 [TEKKUP].
[38] C. Davies, R.F. Langler, C.V.K. Sharma, M.J. Zaworotko, Chem. Commun. (1997) 567 [TEKKUP01].
[39] J. Ellena, G. Punte, N.S. Nudelman, Acta Crystallogr., Sect. C: Cryst. Struct. Commun. 52 (1996) 2929 [TEMCET].
[40] S.A. Chawdhury, Acta Crystallogr., Sect. B 32 (1976) 1069 [TMPSUL10].
[41] Yu.M. Cheban, Yu.A. Simonov, A.A. Dvorkin, V.K. Rotaru, T.I. Malinovskii, Zh. Strukt. Khim. 29 (1988) 191 [VAWFUU].
[42] F. Nowshad, M. Ul-Haque, J. Chem. Soc., Perkin Trans. 2 (1976) 623 [ADCPME].
[43] S. Rantsordas, M. Perrin, Acta Crystallogr., Sect. B 38 (1982) 1871 [BEWJUI].
[44] R.B. Wilson, Y.S. Chen, I.C. Paul, D.Y. Curtin, J. Am. Chem. Soc. 105 (1983) 1672 [BUBVEZ].
[45] S.P.N. van der Heijden, W.D. Chandler, B.E. Robertson, Can. J. Chem. 53 (1975) 2121 [CBYMBZ].
[46] V.K. Bel'skii, V.K. Rotaru, M.M. Kruchinin, Kristallografiya 28 (1983) 695 [CEHCOH].
[47] E.J.W. Whittaker, Acta Crystallogr. 6 (1953) 714 [CLHOPM].
[48] R. Perrin, R. Lamartine, J. Vicens, M. Perrin, A. Thozet, D. Hanton, R. Fugier, New J. Chem. (Nouv. J. Chim.) 10 (1986) 179 [CUJVUY10].
[49] S. Tandel, H. Zhang, N. Qadri, G.P. Ford, E.R. Biehl, J. Chem. Soc., Perkin Trans. 1 (2000) 587 [CUQWIU].
[50] L.A. Chetkina, V.E. Zavodnik, V.K. Bel'skii, I.G. Arzamanova, M.I. Naiman, Ya.A. Gurvich, Zh. Strukt. Khim. 25 (1984) 109.
[51] U. Siriwardane, S.P. Khanapure, S.S.C. Chu, E.R. Biehl, Acta Crystallogr., Sect. C: Cryst. Struct. Commun. 44 (1988) 200 [FUYHOW].
[52] L.A. Chetkina, V.E. Zavodnik, V.K. Bel'skii, I.G. Arzamanova, Ya.A. Gurvich, Zh. Strukt. Khim. 27 (1986) 114 [GANVAS].
[53] U. Siriwardane, S.P. Khanapure, S.S.C. Chu, E.R. Biehl, Acta Crystallogr., Sect. C: Cryst. Struct. Commun. 44 (1988) 374 [GAPFOS].
[54] B. Chaudhuri, A. Hargreaves, Acta Crystallogr. 9 (1956) 793 [HODURM].
[55] L.A. Chetkina, V.E. Zavodnik, V.K. Bel'skii, A.N. Sobolev, I.G. Arzamanova, Ya.A. Gurvich, R.M. Popova, Zh. Strukt. Khim. 30 (1989) 147 [JEMTEA].
[56] P. Ganis, B. di Blasio, C. Scippa, G. Montando, S. Caccanese, Cryst. Struct. Commun. 5 (1976) 233 [MBCDPM].
[57] S. Rantsordas, M. Perrin, A. Thozet, Acta Crystallogr., Sect. B 34 (1978) 1198 [MYCMPP].
[58] G. Ferguson, R. McCrindle, A.J. McAlees, Can. J. Chem. 67 (1989) 779 [SAXXOE].
[59] J. Frey, Z. Rappoport, J. Am. Chem. Soc. 118 (1996) 5169 [TAXGUU].
[60] H. Nakai, T. Saito, M. Yamakawa, Acta Crystallogr., Sect. C: Cryst. Struct. Commun. 44 (1988) 2117 [VABDOR].
[61] A. Cousson, J. Lelievre, A.P. Chatrousse, F. Terrier, P.G. Farrell, Acta Crystallogr., Sect. C: Cryst. Struct. Commun. 49 (1993) 609 [WACGOW].
[62] Rajnikant, D.J. Watkin, G. Tranter, Acta Crystallogr., Sect. C: Cryst. Struct. Commun. 51 (1995) 2388 [ZEXTEB].
[63] J.C. Barnes, J.D. Paton, J.R. Damewood Jr., K. Mislow, J. Org. Chem. 46 (1981) 4975 [ZZZMKS01].
[64] F.H. Allen, O. Kennard, Chem. Des. Automat. News 8 (1993) 31.
[65] A. Anwer, R. Lovell, A.H. Windle, in: R.J. Roe (Ed.),

Computer Simulation of Polymers, Prentice Hall, Englewood Cliffs, NJ, 1991 chapter 3.
[66] M.P. Makowski, Comput. Polym. Sci. 3 (1993) 1.
[67] J. Kendrick, J. Chem. Soc., Faraday Trans. 86 (1990) 3995.
[68] T. Straßner, Can. J. Chem. 75 (1997) 1011.
[69] M. Feigel, J. Mol. Struct. (Theochem.) 366 (1996) 83.
[70] H. Ishii, I. Ando, S. Ando, NMR prep. Jpn., 37 (1998) 332.
[71] D.F. Ewing, Org. Magn. Reson. 12 (1979) 499.